ACS APPLIED MATERIALS & INTERFACES

Research Article

www.acsami.org

Wear-Resistant and Antismudge Superoleophobic Coating on Polyethylene Terephthalate Substrate Using SiO_2 Nanoparticles

Yongxin Wang and Bharat Bhushan*

Nanoprobe Laboratory for Bio- & Nanotechnology and Biomimetics (NLBB), The Ohio State University, 201 W. 19th Avenue, Columbus, Ohio 43210-1142, United States

ABSTRACT: It is of interest to create superoleophobic surfaces that exhibit high oil contact angle, low contact angle hysteresis, high wear resistance, antismudge properties, and optical transparency for industrial applications. In the superoleophobic surfaces developed to date, the mechanical durability data is lacking. By dip-coating polyethylene terephthalate substrate with hydrophobic SiO_2 nanoparticles and methylphenyl silicone resin, followed by O_2 plasma treatment and vapor deposition of 1*H*,1*H*,2*H*,2*H*-perfluorooctyl-trichlorosilane, a durable superoleophobic surface was fabricated. The degree of superoleophobicity was found to be dependent on the particle-to-binder ratio. The coatings were found to exhibit wear resistance on microscale and macroscale, antismudge properties, and transparency.

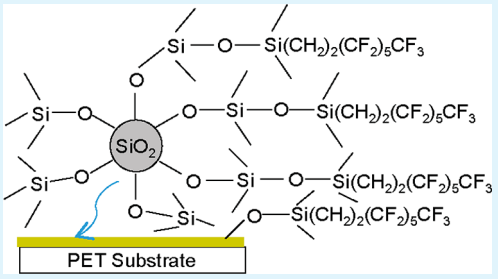

KEYWORDS: *superoleophobic, wear-resistant, antismudge, fluorobinder, nanoparticles*

1. INTRODUCTION

Superoleophobic surfaces, having contact angle (CA) greater than 150° combined with contact angle hysteresis (CAH) or tilt angle (TA) of 2°−10° with liquids with surface tension on the order of 20−27 mN/m, have attracted interest within the scientific community and industry for their unique characteristics such as self-cleaning, antifouling, and drag reduction.[1−9] For industrial applications, superoleophobic surfaces are often required to be wear-resistant, antismudge (fingerprint resistance), and transparent. Examples of applications include windows, solar panels, electronic touch screens, and computer displays.[6]

The wetting behavior of a droplet on a substrate depends on surface chemistry and surface roughness. On a rough surface, a composite wetting where the droplet sits on peaks of roughness features and air pockets fill the gaps in between (so-called Cassie−Baxter regime[10]) is preferred for the design of a superoleophobic coating. A high fraction of liquid−air contact area will lead to high CA and low CAH.[6,10] Many attempts to fabricate superoleophobic coatings have been made. The updated Table 1 from Muthiah et al.[8] provides a summary of reported fabrication attempts on resin binder, nanoparticle or substrate geometry, solvent, deposition method, substrates, and coating thickness with their CA, CAH, TA values, and mechanical durability.

Fluorinated monoalkylphosphate has been deposited onto a rough anodized aluminum surface by immersion coating.[11] Fluorinated acrylic copolymer has been used with TiO_2,[1] ZnO,[12] and SiO_2[13] nanoparticles as well as carbon nanofibers[14] to form nanocomposites and spray- or spin-coated on Si wafer, glass, and sandpaper. A dual-layered coating has been fabricated on glass by dip- and spray-coating of fluorinated acrylic copolymer with hydrophobic SiO_2 nanoparticles.[8] FluoroPOSS has been electrospun to produce beads-on-fibers structures.[15] FluoroPOSS has also been dip-coated onto Si with microhoodoo geometry,[15] and electrospun on stainless steel wire meshes.[16] The electrospun-coated stainless steel wire meshes showed a CA higher than 150° for polydimethylsiloxane (PDMS) droplet. (Heptadecafluoro-1,1,2,2-tetrahydrodecyl)triethoxysilane with fluorinated SiO_2 nanoparticles has been spin-coated on glass,[17] and (heptadecafluoro-1,1,2,2-tetrahydrodecyl)-trimethoxysilane with SiO_2 nanoparticles has been immersion-coated on cotton fabrics.[18]

Poly(tetrafluoroethylene) (PTFE) amorphous fluoropolymer has been electrospun to produce core−sheath fibers with polycaprolactam (PCL)[19] and spin-coated on micropatterned PDMS surface.[20] Jung and Bhushan[3] have deposited *n*-perfluoroeicosane on micropatterned Si with pillars by thermal evaporation. Zhang and Seeger[21] used a dual-layered approach, where Si nanofilaments were grown on glass from trichloro(methyl)silane as the first layer and then 1*H*,1*H*,2*H*,2*H*-perfluorodecyltrichlorosilane was deposited on the glass by immersion coating as the second layer. Perfluorooctanoic acid and copper acetate has been used to form copper perfluoro-octanoate, which was spray-coated on glass.[22]

He et al.[5] has also fabricated a dual-layered coating, where the glass was spin-coated with PDMS/SiO_2 and sintered to degrade the PDMS, and then 1*H*,1*H*,2*H*,2*H*-perfluorooctyl-trichlorosilane (perfluorotrichlorosilane) was deposited on this glass by immersion coating. Zhao et al.[23] has deposited perfluorotrichlorosilane on micropatterned Si wafer with pillars by molecular vapor deposition. Deng et al.[24] fabricated a triple-layered coating,

Received: October 17, 2014
Accepted: December 16, 2014
Published: December 16, 2014

DOI: 10.1021/am5067755
ACS Appl. Mater. Interfaces 2015, 7, 743−755

Table 1. Literature Review on Binder and Nanoparticle Systems, Deposition Methods, and Substrates Used in Fabrication of Superoleophobic Surfaces[a]

resin binder	nanoparticle or substrate geometry, solvent, deposition method, substrate, coating thickness[b]	CA[c] (deg)	summary and comments[b]
fluorinated monoalkylphosphate	anodized aluminum surface, ethanol, immersion coating[11]	CA (rapeseed oil) 150	A rough anodized aluminum substrate used.
		CA (water) 150	
fluorinated acrylic copolymer in water (Zonyl 8740 or Capstone ST-100—Dupont Co.)	TiO_2 nanoparticles (20−50 nm), water, spray coating on Si wafer[1]	CA (ethylene glycol) 144	Larger P−B ratio gives higher CA.
		CA (water) 164	
	ZnO nanoparticles (50 nm), water/acetone, spray coating on glass[12]	CA (hexadecane) 154	P−B ratio at 3.3 yielded most superoleophobic and 1.6 yielded most superhydrophobic surfaces.
		CAH (hexadecane) 6	
		CA (water) 168	
	SiO_2 nanoparticles (30−50 nm) by sol−gel method, water, spin coating on Si wafer, 6 μm thick[13]	CA (ethylene glycol) 165	On the basis of P−B ratios, F/Si atomic ratio of 2.1 found to be best for water and ethylene glycol repellency.
		CAH (ethylene glycol) 3	
		CA (water) 168	
		CAH (water) 2	
	carbon nanofibers (CNF) (100 nm dia., length ≈ 130 μm), water/acetone + formic acid, spray coating on glass and sand paper, 5 μm thick[14]	CA (mineral oil) 164	CNF with heat transfer characteristics may find applications in fabricating icephobic surfaces.
		TA (mineral oil) 9	
		CA (water) 164	
		TA (water) 5	
	SiO_2 nanoparticles (55 nm), acetone, dual-layered coating (dip coating fluoroacrylic and spray coating fluoroacrylic + SiO_2), glass[8]	CA (hexadecane) 147	P−B ratio at 0.6 yielded most superomniphobic coating.
		CAH (hexadecane) 12	
		CA (ethylene glycol) 153	
		CAH (ethylene glycol) 11	
		CA (water) 160	Mechanically durable and antismudge.
		CAH (water) 9	
1*H*,1*H*,2*H*,2*H*-heptadecafluorodecyl modified polyhedral oligomeric silsesquioxane) (fluoroPOSS)	fluoroPOSS, poly(methyl methacrylate) (PMMA) and Asahiklin AK-225 (consists of 3,3-dichloro-1,1,1,2,2-pentafluoropropane and 1,3-dichloro-1,1,1,2,3-pentafluoropropane), electrospinning to produce fibers (bead size 10−20 μm)[15]	CA_{adv} (hexadecane) 156	A blend of hydrophilic PMMA and low energy fluoroPOSS is used to generate re-entrant surfaces.
		CAH (hexadecane) 6	
		TA (hexadecane) 5	
	fluoroPOSS and Asahiklin AK-225 by dip coating on Si wafer with microhoodoo re-entrant geometry (width = 10 μm, spacing = 20 μm and height = 7 μm) silanized[15]	CA_{adv} (hexadecane) > 150	Re-entrant geometry explored.
	Electrospun coating of cross-linked PDMS/fluoroPOSS on stainless steel wire meshes, Asahiklin 225/methylformamide[16]	CA (PDMS) > 150	Hierarchical scales of re-entrant texture.
		CAH (PDMS) 6	
		TA (PDMS) 1.5	Chemical resistant to various liquids.
		CA (hexadecane) > 150	
		CAH (hexadecane) 5	
		TA (hexadecane) 1.5	
(heptadecafluoro-1,1,2,2-tetrahydrodecyl) triethoxysilane (Gelest Inc.) or 1*H*,1*H*,2*H*,2*H*-perfluorodecyltriethoxysilane (Degussa Chemical Company)	fluorinated SiO_2 nanoparticles, isopropanol, spin coating, glass[17]	CA (xylene) 141	Sol−gel method was used for fabrication of fluorinated SiO_2 nanoparticles.

ACS Appl. Mater. Interfaces 2015, 7, 743−755
DOI: 10.1021/am5067755

Table 1. continued

resin binder	nanoparticle or substrate geometry, solvent, deposition method, substrate, coating thickness[b]	CA[c] (deg)	summary and comments[b]
		CA (diiodomethane) 159	
		CA (water) 168	
(heptadecafluoro-1,1,2,2-tetrahydrodecyl) trimethoxysilane (Gelest Inc.) or 1*H*,1*H*,2*H*,2*H*-perfluorodecyltrimethoxysilane (Sigma-Aldrich)	SiO_2 nanoparticles (~150 nm), acetone, saturating cotton fabrics in solution and irradiating with microwave-assisted synthetic techniques[18]	CA (hexadecane) 137	Repel liquid and adsorb organic vapors from liquid droplets. High affinity for 3-hepten-2-one vapor.
		CA (water) 157	
PTFE amorphous fluoropolymer (Teflon AF 2400 − Dupont Co.)	coaxial-electrospinning of polycaprolactam (PCL)/2,2,2-trifluoroethanol core and Teflon AF 2400/FC-75 (perfluorocarbon) sheath fibers (~2 μm in diameter) on aluminum foil[19]	CA (hexadecane) 138	Teflon AF 2400 is made electrospinnable by coaxial-electrospinning process using PCL.
		CA (ethylene glycol) 155	
		CA (water) 160	
		CAH (water) 4	
		TA (water) 7	
	PTFE amorphous fluoropolymer and FC-40 (perfluorocarbon) spin coating on polydimethylsiloxane (PDMS) surface with inverse-trapezoid (height = 12 μm, width = 26 μm, pitch = 40 μm)[20]	CA (methanol) 135	Transparent, flexible, re-entrant surface was explored.
		CA (water) 153	
		CAH (water) 18	
n-perfluoroeicosane (268828, Sigma-Aldrich)	thermal evaporation on to micropatterned Si wafer with cylindrical pillars (diameter = 14 μm, height = 30 μm and pitch = 23 μm)[3]	CA (hexadecane) 133	A model for predicting CA of water and oil droplets evaluated.
		CA (water) 160	
1*H*,1*H*,2*H*,2*H*-perfluorodecyltrichlorosilane (ABCR Germany)	Si nanofilaments grown on trichloromethylsilane treated glass, dry toluene, immersion coating[21]	CA (decane) 163	Optically transparent.
		CA (dodecane) 167	Stable against outdoor conditions, ozone, UV light, basic and acid.
		CA (hexadecane) 174	
perfluorooctanoic acid	spray coating of copper perfluorooctanoate from perfluorooctanoic acid and copper acetate on glass, ethanol, 150 μm thick[22]	CA (dodecane) 150	Apply to any surface.
		CAH (dodecane) 23	Stable to high speed rotation (4000 rps). Fragile to scratch but easy to repair by respray.
		CA (hexadecane) 155	
		CAH (hexadecane) 22	
trichloro(1*H*, 1*H*, 2*H*, 2*H*-perfluorooctyl)silane, or tridecafluoro-1,1,2,2-tetrahydrooctyltrichlorosilane, or 1*H*,1*H*,2*H*,2*H*-perfluorooctyl-trichlorosilane (Sigma-Aldrich, Gelest Inc., ABCR, or Alfa Aesar Inc.)	SiO_2 nanoparticles (10−30 nm), spin coating of PDMS/SiO_2 on glass and sinter to degrade PDMS, toluene, immersion coating[5]	CA (diiodomethane) 141	Optically transparent.
		TA (diiodomethane) 6	Thermally stable to 95 °C and stable to outdoor condition. Poor durability to ultrasonic bath damage and adhesive tape peeling.
		CA (water) 153	
		TA (water) 6	
	molecular vapor deposition on micropatterned Si wafer with cylindrical pillars (diameter = 2.7 μm, height = 7 μm, and pitch = 6 μm)[23]	CA (hexadecane) 158	Various fluorosilane coatings explored on patterned surface.
		TA (hexadecane) 10	
		CA (water) 156	
		TA (water) 10	
	CVD of tetraethoxysilane on glass with carbon particles (40 nm) and calcination to form a silica shell first and then CVD of resin binder, ~8 μm thick[24]	CA (hexadecane) 156	Optically transparent.

ACS Appl. Mater. Interfaces 2015, 7, 743−755
DOI: 10.1021/am5067755

Table 1. continued

resin binder	nanoparticle or substrate geometry, solvent, deposition method, substrate, coating thickness[b]	CA[c] (deg)	summary and comments[b]
		TA (hexadecane) 5	Limited resistant to sand abrasion (5 min) and coating peeled off by adhesive tape. Thermally stable to 400 °C.
		CA (ethylene glycol) 160	
		TA (ethylene glycol) 2	
		CA (water) 165	
		TA (water) 1	
	CVD of resin binder on SiO_2 aerogel (nanoparticle network), 1−2 mm thick[25]	CA_{adv} (mineral oil) 168	Mechanically durable to sand abrasion. After sandpaper abrasion, CAH decreased to 14 for mineral oil and 1 for water.
		CAH (mineral oil) 38	
		TA (mineral oil) 10	
		CA_{adv} (water) 172	
		CAH (water) 22	
		TA (water) 2	
fluorinated 3,4-ethylenedioxypyrrole (EDOP) monomer	electropolymerization onto Si arrays of cylindrical micropillars (13 mm dia., 25 μm height, 40 μm distance between cylinders, photolithography and coated by gold first)[4]	CA_{adv} (hexadecane) 155	Super oil-repellency.
		CAH (hexadecane) 40	
		TA (hexadecane) 26	
		CA_{adv} (sunflower oil) 155	
		CAH (sunflower oil) 4	
		TA (sunflower oil) 3	
	electrochemical polymerization of monomer with micro/nano roughness on gold plate[26]	CA (hexadecane) 150	EDOP with different chain length found to affect surface morphology of polymer film.
		CAH (hexadecane) 22	
		TA (hexadecane) 11	
		CA (water) 157	
		CAH (water) 2	
		TA (water) 1	
fluorinated polyurethane	fluorinated multiwalled carbon nanotubes (MWCNTs, 20−40 nm diameter and 30−50 mm length), acetone/toluene, spray coating on glass[27]	CA (hexadecane) 152	A coralline-like structure formed.
		CA (water) 162	
fluoropolymer (copolymer of ethylene, tetrafluoroethylene and perfluoromethylvinyl ether, and a cure site monomer) (Viton ETP-600S—Dupont Co.)	SiO_2 aggregates (92 m^2/g) (fluoroalkyl-functionalized), Asahiklin AK-225G (1,3-dichloro-1,2,2,3,3-pentafluoropropane), spray coating on Si wafer[28]	CA_{adv} (hexadecane) 155	On the basis of various particle-to-binder mass fractions, 80/20 (w/w) yielded maximum hexadecane CA values.
		TA (hexadecane) 25	
		CA_{adv} (rapeseed oil) 158	
		TA (rapeseed oil) 8	
		CA_{adv} (water) 165	
		TA (water) 1	

[a]Contact angle (CA), contact angle hysteresis (CAH), and tilt angle (TA) values and mechanical durability (adapted from Muthiah et al.[8]). [b]Particle-to-binder ratio (P−B); chemical vapor deposition (CVD). [c]Surface tension of DI water = 72.0 mN/m, ethylene glycol = 48.0 mN/m, hexadecane = 27.0 mN/m, methanol = 22.1 mN/m,[44] mineral oils, rapeseed oil = 30−35 mN/m,[6] sunflower oil ≈ 31 mN/m,[4] PDMS= 20 mN/m, xylene = 29.5 mN/m,[16] diiodomethane = 50.8 mN/m, dodecane = 25.4 mN/m, decane = 23.8 mN/m.[21]

ACS Appl. Mater. Interfaces 2015, 7, 743−755
DOI: 10.1021/am5067755

where glass substrate was coated with a soot layer (first layer), covered with a silica shell from tetraethoxysilane (second layer), and coated with perfluorotrichlorosilane by chemical vapor deposition (CVD, third layer). Perfluorotrichlorosilane has also been CVD-coated on SiO_2 aerogel.[25] Fluorinated 3,4-ethylenedioxypyrrole (EDOP) monomer has been electropolymerized on Si arrays coated with gold[4] and on gold plate to create micro- and nanoroughness.[26] Fluorinated polyurethane with fluorinated multiwalled carbon nanotubes (MWCNTs) has been spray-coated on glass,[27] and fluoropolymer Viton ETP-600S with SiO_2 aggregates has been spray-coated on Si wafer.[28]

The liquids used for characterizations, mechanical durability, antismudge properties, transparency, and other relevant information are also listed in Table 1. The liquids include deionized (DI) water with a surface tension of 72.0 mN/m and various organic liquids with a range of surface tension from 20−50.8 mN/m, as listed at the bottom of Table 1. For most liquids, CA values are greater than 150° with CAH and TA values less than 10°. Mechanical durability data of some coatings are reported, while the others are lacking. The CVD-coated SiO_2 aerogel by Jin et al.[25] was reported to be superoleophobic but with high CAH making it undesirable for self-cleaning. After a sand abrasion test, they reported that the coating had no degradation in wettability. Yang et al.[22] reported their coating to be susceptible to scratch. The coating produced by He et al.[5] showed poor durability to ultrasonic bath damage, and part of the coating material can be peeled off with adhesive tape. Deng et al.[24] and Ge et al.[29] reported their coatings were eroded after sand abrasion. Muthiah et al.[8] reported a coating with some durability and antismudge properties. However, some aggregated nanoparticles were able to be rubbed off with a microfiber cloth. Note that they were the only group to study antismudge properties. Transmittance range of 80−90% implying limited transparency has been reported by Im et al.,[20] He et al.,[5] Zhang and Seeger,[21] and Deng et al.[24] The published data suggest that the mechanical durability of superoleophobic coatings needs to be improved. There exists only one paper on antismudge properties.

The objective of this research is to develop a highly durable superoleophobic coating with antismudge properties and transparency. To develop superoleophobic coatings, the surface energy of the coatings needs to be lower than the surface tension of liquids of interest. To achieve this, fluorinated compounds need to be used, which have generally poor adherence and poor mechanical durability.[5,8,22,29] The strategy of developing a highly durable coating with antismudge properties and transparency is to use a dual-layer approach. The first layer was selected to provide high durability and optical transparency. The second layer was selected to provide superoleophobicity and antismudge properties. The results of this study are the subject of this paper.

2. EXPERIMENTAL DETAILS

In this research, a dual-layer coating was fabricated on poly(ethylene terephthalate) (PET) substrate as shown in Figure 1. PET substrate was selected because of its transparency, flexibility, low price, and light weight, which are important for electronic and industrial applications. For the first layer, a durable binder-nanoparticle nanocomposite was selected to provide the mechanical durability and was deposited by dip coating. Silicone-based binders have been used for fabrication of superoleophobic coatings by He et al.[5] and Deng et al.[24] Silicone-based and epoxy binders have been used for fabrication of superhydrophobic coatings by various researchers, for example, Ebert and Bhushan.[30,31] In this study, methylphenyl silicone resin was selected

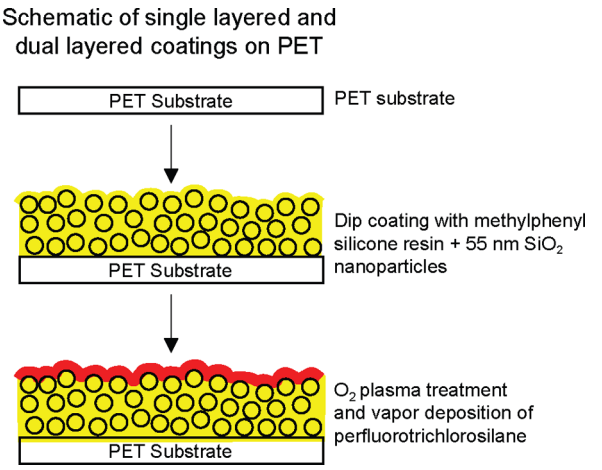

Figure 1. Schematic of single layer of dip-coated PET and dual layer of vapor deposition of perfluorotrichlorosilane on plasma-treated, dip-coated PET.

because it is known to be durable and offer strong adhesion between nanoparticles and substrate.[30] Next, hydrophobic SiO_2 nanoparticles with methyl groups were selected because they have high hardness to resist wear and high visible transmittance to provide transparency. Dip-coating technique was selected because it is simple, versatile, and provides a uniform coating.[6]

Next, for the second layer, a chemically active fluorinated binder was selected. On the basis of our previous experience, prevalence of binders used, and commercial availability, we narrowed our selections to fluorinated acrylic copolymer,[1,8,12−14] PTFE amorphous fluoropolymer,[19,20] and perfluorotrichlorosilane.[5,23−25] The binder perfluorotrichlorosilane was selected based on oil CA and durability. As mentioned earlier, fluorinated compounds generally have poor adherence, and effective attachment requires the substrates to be chemically active. O_2 plasma treatment is known to be surface sensitive changing the properties at the surface without affecting those in the bulk coating, and it has been used in many applications.[21,32,33] Therefore, O_2 plasma treatment was used to create active hydroxyl groups (−OH) at the surface of the first layer to form covalent bonds with perfluorotrichlorosilane as the second layer. Perfluorotrichlorosilane may also hydrolyze when in contact with water, and this would promote its condensation. Perfluorotrichlorosilane was deposited using dip and vapor approaches.

2.1. Coating Procedure. Before coating, PET substrate (100 μm thick, obtained from Dexerials Corporation, Japan, formerly Sony Corp. Chemical Division) was cleaned in isopropyl alcohol (IPA, Fisher Scientific) with bath sonication (45 kHz frequency, Fischer Scientific, model FS5) for 10 min. Then, it was rinsed with DI water and allowed to air-dry. SiO_2 nanoparticles (Aerosil RX 50, functionalized by Evonik Industries) with an average diameter of 55 nm were dispersed in a mixture of 30 mL of 40% tetrahydrofuran (THF, Fisher Scientific)/60% IPA (by volume), followed by sonication for 4 min with Branson Sonifier 450A (20 kHz frequency at 35% amplitude). Then, 150 mg of methylphenyl silicone resin (SR355S, Momentive Performance Materials) was added and sonicated for an additional 4 min to form a dip-coating solution.[30] Several concentrations of SiO_2 nanoparticles were used −2.5, 5, 10, 15, 17.5, and 20 mg/mL. PET substrate was dipped into the solution and withdrawn immediately at a speed of 100 mm/min. Coated samples were dried in oven at 40 °C for 10 min to remove the remaining solvent.

Then, the dip-coated PET was treated with O_2 plasma (Plasmalab System 100, Oxford Instruments) at an O_2 flow rate of 10 sccm and a power of 100 W for 10 min (chamber pressure 15 mTorr). The treated PET was placed in a desiccator for short-term storage and transport. Perfluorotrichlorosilane (448931, Sigma-Aldrich) with a volume of 0.1 mL was vapor-deposited on the dip-coated PET in a vacuum chamber at 30 mTorr. A vapor deposition time of 16 h was used,

DOI: 10.1021/am5067755
ACS Appl. Mater. Interfaces 2015, 7, 743−755

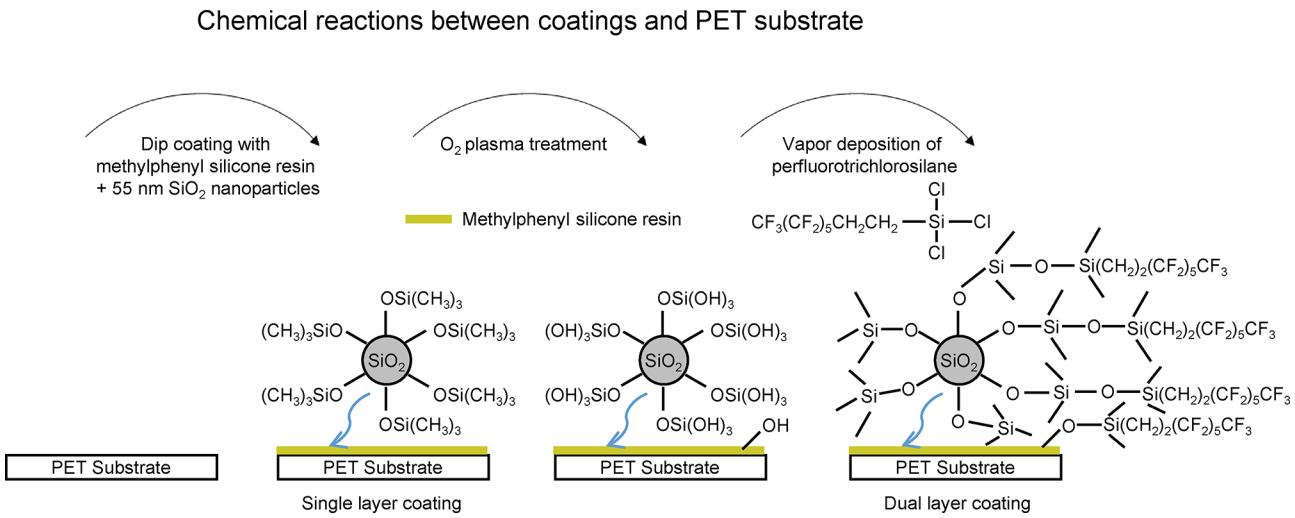

Figure 2. Schematics of chemical reactions between coating and PET substrate after plasma treatment.

which provided a uniform coating. For comparison, dip coating of perfluorotrichlorosilane was also carried out (0.5 or 2 wt % in hexanes for 5 min, Mallinckradt). The samples were dried at 120° for 5 min.

To explain the mechanism, schematics of the chemical reactions between the coating and the PET substrate with O_2 plasma treatment are shown in Figure 2.[34] Methylphenyl silicone resin and hydrophobic SiO_2 nanoparticles were dip-coated on PET as a single-layer coating (physically bonding). O_2 plasma was carried out on the single layer to obtain hydroxyl groups (−OH) on both components. Perfluorotrichlorosilane condensed with hydroxyl groups (−OH) formed covalently attached, cross-linked polymeric layers as a dual-layer coating (chemically bonding).

2.2. Characterization. CA, CAH, TA, surface topography, coating thickness, wear resistance on microscale and macroscale, and antismudge properties were measured.

2.2.1. Wettability with CA, CAH, and TA. CA, CAH, and TA of commonly used liquids of scientific interest were measured with a standard automated goniometer (Model 290, Ramé-Hart Inc.). These liquids include DI water (surface tension = 72.0 mN/m), ethylene glycol (Mallinckradt, 48.0 mN/m), and hexadecane (Alfa Aesar, 27.0 mN/m). The static CA was measured by depositing a 5 μL drop onto a sample with a microsyringe and capturing the image of a profile of the liquid−air interface with DROPimage software. CAH was calculated from advancing and receding CAs, which were measured on an inclined surface. TA refers to the angle where a 5 μL drop just began to roll off the surface of a sample. All angles were averaged over three measurements of a sample on different areas.

2.2.2. Surface Topography and Coating Thickness. The surface topography of each sample was imaged using a D3000 Atomic Force Microscopy (AFM) with a Nanoscope IV controller (Bruker Instruments). A Si, N-type (Si_3N_4) tip with Al coating (resonant frequency f = 66 kHz, k = 3 N/m, AppNano) in tapping mode was used. The scanning area was 1 × 1 μm^2. Root mean square roughness (RMS) and peak-to-valley (P−V) distance values were obtained.

Coating thickness was measured with a step technique. One half of the substrate was covered with a sticky tape before coating, and the tape was removed after the coating process to create a step. IPA was used to remove the residual of the sticky tape. An area of 25 × 25 μm^2 including the step was scanned with AFM to obtain coating thickness.

2.2.3. Wear Resistance. Wear experiments were performed using an AFM and a ball-on-flat tribometer.[35] Microscale wear was measured with AFM, and the coating was worn using a borosilicate ball with a radius of 15 μm mounted on a Si cantilever (resonant frequency f = 150 kHz, spring constant k = 7.4 N/m, All-In-One) in contact mode. An area of 50 × 50 μm^2 was worn for one cycle (round trip) at a load of 10 μN. The changes in morphology of the coatings were compared before and after wear, where the surface topography of 100 × 100 μm^2 in area was imaged with a Si tip in tapping mode.

Macroscale wear was performed with a ball-on-flat tribometer.[36] A sapphire ball with a radius of 1.5 mm was fixed in a stationary holder. A load of 10 mN was applied normal to the coated surface, and the tribometer was set into reciprocating motion for 100 cycles (round trip). Stroke length was 6 mm, and average linear speed was 1 mm/s for tests performed. Surfaces were imaged before and after the tribometer wear experiment using an optical microscope with a CCD camera (Nikon Optihot-2).[31]

The contact pressures for wear using AFM and tribometer were calculated based on Hertz analysis.[36] The elastic modulus of silicone rubber at 50% elongation, 0.5 GPa,[37] was used to estimate the elastic modulus of the dual-layer coating, and a Poisson's ratio of 0.5 was used (estimated). The elastic modulus of nanocomposite coating is expected to be higher, so an underestimated pressure will be obtained with the selected modulus. The elastic modulus of 70 GPa and Poisson's ratio of 0.2 were used for borosilicate ball for microscale wear using AFM.[38] The elastic modulus of 390 GPa and Poisson's ratio of 0.23 were used for sapphire ball for macroscale wear using tribometer.[37] The mean contact pressures were calculated as 10.36 and 4.83 MPa for wear using AFM and ball-on-flat tribometer, respectively. As mentioned earlier, the microscale wear using AFM was performed for one cycle; the macroscale wear using tribometer was performed for 100 cycles. Comparing with wear using AFM, the wear using tribometer with multiple cycles can cause a relatively high degree of damage to the dual-layer coating even though the mean contact pressures are comparable.

2.2.4. Antismudge Properties. The antismudge properties were tested with a lab-designed instrument.[8,39] The sample was first contaminated with silicon carbide (SiC, 400 mesh particle size, 357391, Sigma-Aldrich) in a glass chamber (0.3 m diameter and 0.6 m high) by blowing 1 g of SiC powder onto a sample at 10 s at 300 kPa and allowing it to settle for 30 min. With the antismudge apparatus, the contaminated sample was secured on a stage. Then, a hexadecane (oil)-impregnated microfiber wiping cloth was glued to a horizontal glass rod fixed on a cantilever (radius 0.5 mm) above the sample. As the cloth was brought in contact with the sample, the microfiber cloth was set to rub the contaminated sample under a load of 5 g for 1.5 cm at a speed of ~0.2 mm/s. Photographs were taken using an optical microscope with a CCD camera (Nikon, Optihot-2). The removal and transfer of nanoparticles by the cloth was compared before and after tests.

3. RESULTS AND DISCUSSION

Wettability of coated surfaces is presented with CA, CAH, and TA, and optimization of the particle-to-binder (P−B) ratio of the single layer for CAs of interest is presented. Surface topography and coating thickness values are reported. Next, wear

DOI: 10.1021/am5067755
ACS Appl. Mater. Interfaces 2015, 7, 743−755

resistance and antismudge properties are presented. Finally, the transparency of coated samples is reported and compared with uncoated samples.

3.1. Wettability of Coated Surfaces. The measured CA, CAH, and TA values of water, ethylene glycol, and hexadecane on coated and uncoated PET samples with their relative durability based on AFM experiment are shown in Table 2. The uncoated PET showed hydrophilic and oleophilic wettability with CA 78° ± 2° and 55° ± 2°, CAH 20° ± 2° and 22° ± 2° for water and ethylene glycol, respectively. The uncoated PET substrate was completely wet as a hexadecane droplet was deposited with a CA close to 0°.

3.1.1. Single-Layer Coating. For comparison, in the initial experiments, both hydrophobic and hydrophilic SiO_2 nanoparticles were used. The same procedure was followed with hydrophilic SiO_2 as with hydrophobic SiO_2. Lower CA with hydrophilic nanoparticles were obtained probably because of agglomeration of nanoparticles in the dip-coating solution due to hydrogen bonding between hydroxyl groups (−OH) resulting in a nonuniform coating. Previous research also showed that, compared with hydrophilic SiO_2, hydrophobic SiO_2 had a better dispersion/homogeneity (for lack of hydrogen bonds) and better wear resistance.[40,41] Thus, hydrophobic SiO_2 was selected for this study.

For the single-layer coating, PET was dip-coated with methylphenyl silicone resin and hydrophobic SiO_2 to provide high durability. It is known that P−B ratio affects the wettability,[8] and it needs to be optimized for high CA. Figure 3 shows CA and CAH of water and ethylene glycol on dip coated PET at various P−B ratios. CAs of hexadecane are close to 0° and are not shown in the figure. Dip-coated PET with methylphenyl silicone resin alone showed wettability properties with CA 74° ± 2° and 36° ± 3°, CAH 21° ± 2° and 30° ± 3° for water and ethylene glycol, respectively. The data provided a baseline.

CA with water increases and CAH decreases as P−B ratio increases from 0 to 2.0, and then CA remains higher than 165° as the P−B ratio varies from 2.0 to 4.0. This occurs because, with increasing concentration of nanoparticles, there is an increasing amount of air pockets beneath the water droplets in Cassie−Baxter wetting regime, leading to a high fraction of water−air contact area from P−B ratio of 0−2.0. When the fractional area between water and air has increased to a critical point, ~0.94 at a P−B ratio of 2.0 where our data are coincident with their observation,[31] an increase of nanoparticle concentrations would not increase the fractional water−air area, and thus CA and CAH have not changed.

The ethylene glycol droplets, which have a lower surface tension (48.0 mN/m) compared with water (72.0 mN/m), behaved differently on samples with various P−B ratios. From P−B ratio of 0 to 3.0, CA of ethylene glycol increases, while CAH decreases, associating with an increase of fractional contact area between ethylene glycol and air in Cassie−Baxter wetting regime; from P−B ratio of 3.0 to 4.0, CA of ethylene glycol decreases while CAH increases, associating with a decrease of fractional contact area between ethylene glycol and air. At P−B ratios less than 3.0, addition of nanoparticles results in an increase of surface roughness, which benefits formation of air pockets; at P−B ratios more than 3.0, addition of nanoparticles leads to a rather flat surface with no openings, which is not conducive to formation of air pockets.[8] At a P−B ratio of 3.0, the best wettability was achieved for ethylene glycol with CA 140° ± 3° and CAH 9° ± 2°. The overall goal of optimization was to find the P−B ratio at which the highest CA and

Table 2. Measured Contact Angle (CA), Contact Angle Hysteresis (CAH), and Tilt Angle (TA) Values and Relative Durability for Coated PET Samples at a P−B[a] Ratio of 3.0

samples	DI water (deg)			ethylene glycol (deg)			hexadecane (deg)			relative durability based on AFM experiment	comments
	CA	CAH	TA	CA	CAH	TA	CA	CAH	TA		
PET substrate	78 ± 2	20 ± 2	>90	55 ± 2	22 ± 2	>90	~0	N/A[a]	>90	baseline	hydrophilic
single-layer coating − methylphenyl silicone resin + SiO_2											
dip deposition of methylphenyl silicone resin + SiO_2 (~300 nm thick)	165 ± 2	2 ± 1	2 ± 1	140 ± 3	9 ± 2	>90	~0	N/A[a]	>90	excellent	superhydrophobic oleophobic/oleophilic
single-layer coating − perfluorotrichlorosilane											
dip deposition of perfluorotrichlorosilane (~200 nm thick)	110 ± 2	13 ± 2	>90	95 ± 3	15 ± 2	>90	79 ± 2	16 ± 2	>90	good	hydrophobic oleophobic/oleophilic
vapor deposition of perfluorotrichlorosilane (~200 nm thick)	106 ± 3	14 ± 2	>90	92 ± 4	17 ± 2	>90	76 ± 3	19 ± 2	>90	good	hydrophobic oleophobic/oleophilic
dual-layer coating − methylphenyl silicone resin + SiO_2 + perfluorotrichlorosilane											
dip deposition of perfluorotrichlorosilane (~200 nm thick)	166 ± 2	2 ± 1	2 ± 1	139 ± 2	12 ± 2	>90	42 ± 2	25 ± 2	>90	poor	superhydrophobic oleophobic/oleophilic
vapor deposition of perfluorotrichlorosilane (~200 nm thick)	165 ± 2	2 ± 1	1 ± 1	140 ± 3	10 ± 2	>90	44 ± 2	24 ± 2	>90	excellent	superhydrophobic oleophobic/oleophilic
dual-layer coating − methylphenyl silicone resin + SiO_2 + plasma treatment + perfluorotrichlorosilane											
dip deposition of perfluorotrichlorosilane (~1 μm thick)	166 ± 2	2 ± 1	2 ± 1	151 ± 4	5 ± 3	4 ± 2	146 ± 3	8 ± 2	>90	poor	superhydrophobic superoleophobic
vapor deposition of perfluorotrichlorosilane (~300 nm thick)	170 ± 2	2 ± 1	1 ± 1	165 ± 2	3 ± 2	2 ± 2	153 ± 2	4 ± 2	4 ± 2	excellent	superhydrophobic superoleophobic

[a]Particle-to-binder (P−B) ratio; not applicable (N/A).

DOI: 10.1021/am5067755
ACS Appl. Mater. Interfaces 2015, 7, 743−755

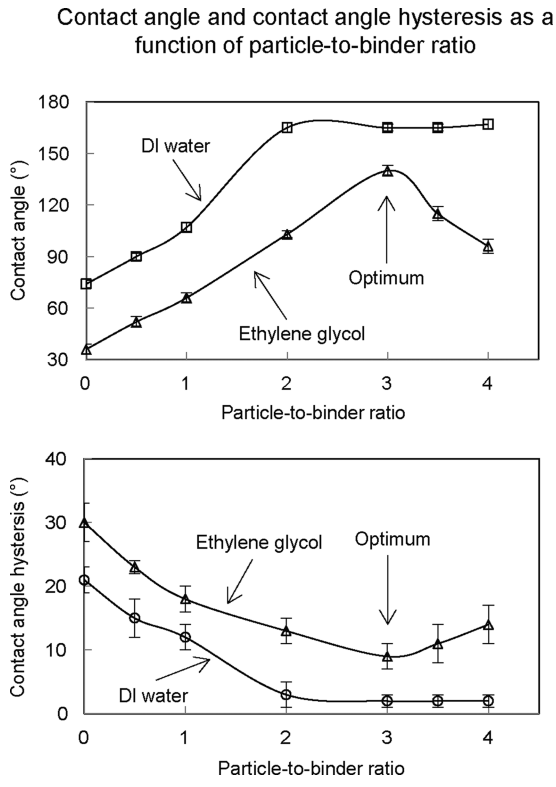

Figure 3. CA and CAH measured using droplets of water and ethylene glycol on single layer of dip-coated PET as a function of P−B ratios. Lines connecting the data are to guide the eyes.

lowest CAH were obtained. Therefore, a P−B ratio of 3.0 was selected for single-layer coating. The measured thickness was approximately 300 nm thick.

At the selected P−B ratio, the coated surface exhibited CA 165° ± 2° and CAH 2° ± 1° for water indicating superhydrophobicity, CA 140° ± 3° and CAH 9° ± 2° for ethylene glycol indicating oleophobicity, and CA close to 0° for hexadecane indicating superoleophilicity. The lack of superoleophobicity could be improved by deposition of perfluorotrichlorosilane.

To select a suitable deposition method for perfluorotrichlorosilane, single-layer coating fabricated by dip-coating and vapor-deposition methods on PET substrate alone were explored. Measured thickness of the coatings was approximately 200 nm. The CA data in Table 2 show that both coated surfaces were hydrophobic as expected. Thus, both deposition methods could be potentially used.

3.1.2. Dual-Layer Coating. Next, dual-layer coatings were deposited using dip and vapor deposition of perfluorotrichlorosilane. In Table 2, CA, CAH, and TA of water on both dip (0.5 wt % in hexanes)- and vapor-deposited coatings (approximately 200 nm thick) were similar to that of single layer of dip-coated PET with methylphenyl silicone resin and SiO_2. A composite wetting was presumably formed with water on these coated surfaces. Ethylene glycol had CA 139° ± 2° and CAH 12° ± 2° for dip deposition of perfluorotrichlorosilane, and CA 140° ± 3° and CAH 10° ± 2° for vapor deposition of perfluorotrichlorosilane, implying insufficient oleophobicity. Especially, CAs of hexadecane droplets were 42° ± 2° and 44° ± 2° for dip- and vapor-deposition of perfluorotrichlorosilane. These values were even lower than those of single-layer dip or vapor deposition of perfluorotrichlorosilane on

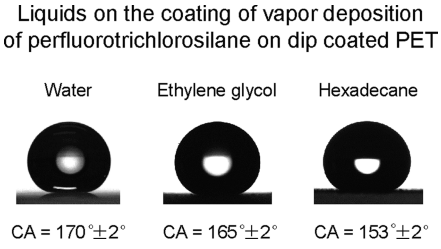

Figure 4. Water, ethylene glycol, and hexadecane droplets deposited on the dual-layer coating.

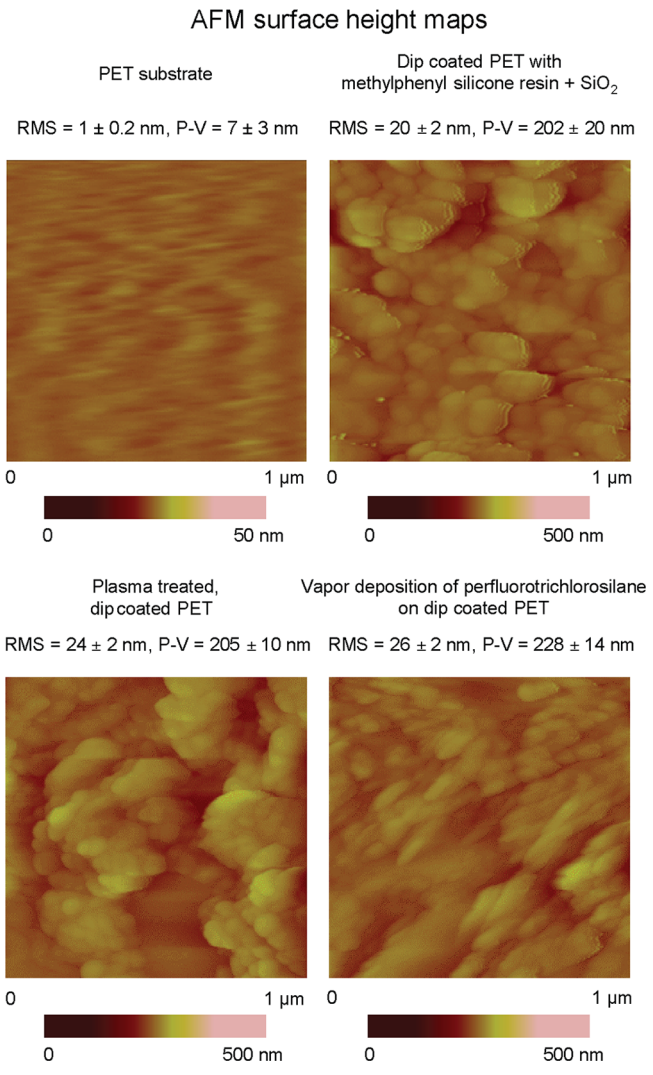

Figure 5. AFM surface height maps with RMS roughness and P−V distance values for PET substrate, single layer of dip-coated PET, dip-coated PET after plasma treatment, and dual-layer coating.

PET alone (CA 79° ± 2° and 76° ± 3°). This suggests that hexadecane droplets were in Wenzel regime. According to Wenzel model, the introduction of surface roughness would make the surface more oleophilic if CA of the liquid on flat surface is less than 90°.[6,42]

The reasons for lack of oleophobicity are the following. In dip deposition, although perfluorotrichlorosilane was able to hydrolyze and condense under the influence of water from ambient environment, there were limited active groups on the single-layer coating that would bond with limited amount of

DOI: 10.1021/am5067755
ACS Appl. Mater. Interfaces 2015, 7, 743−755

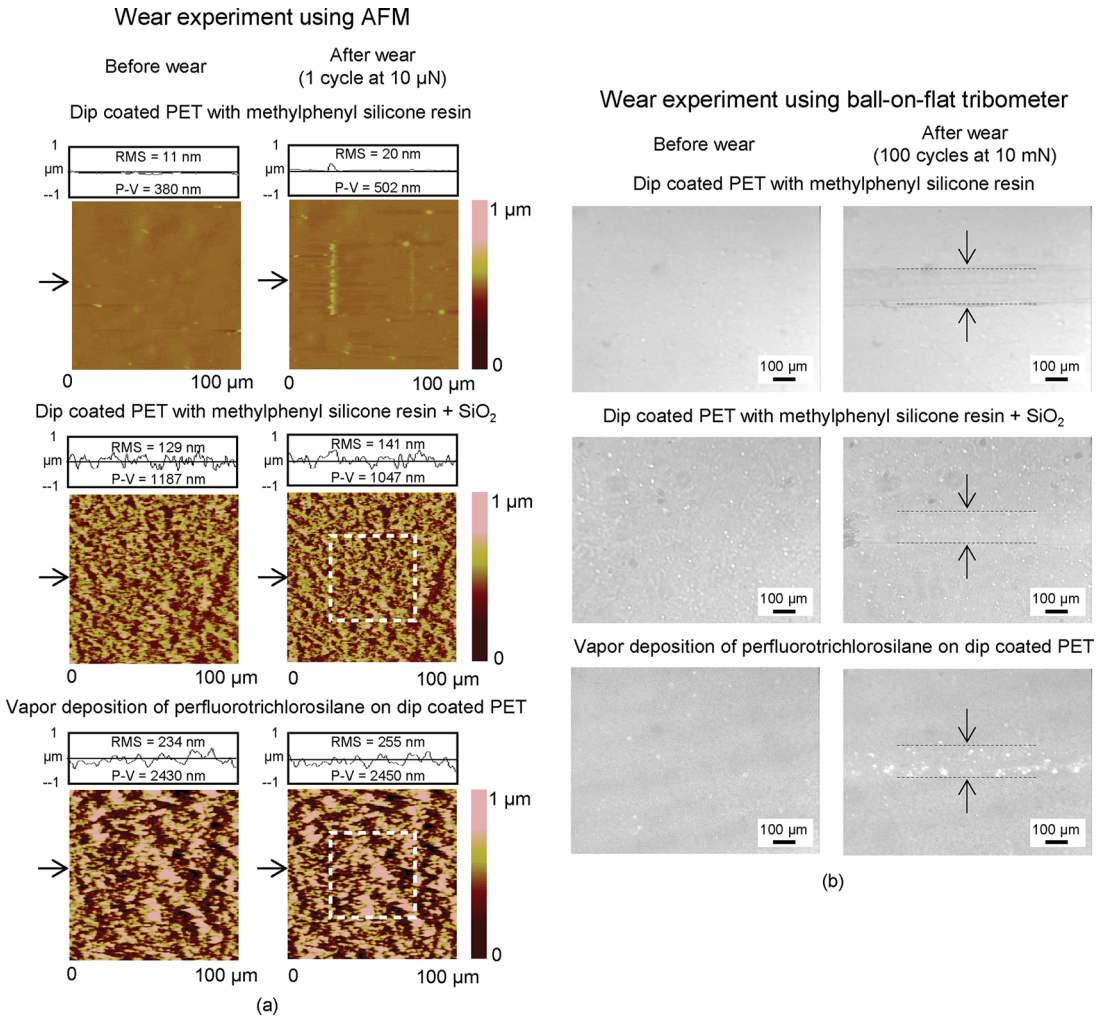

Figure 6. (a) Surface height maps and sample surface profiles (locations indicated by arrows) of samples before and after AFM wear experiment (10.36 MPa). (b) Optical micrographs of samples before and after wear experiment using ball-on-flat tribometer (4.83 MPa).

perfluorotrichlorosilane resulting in less oleophobicity. In vapor deposition, this was also due to insufficient coverage of perfluorotrichlorosilane for lack of active groups, and hydrolysis was restricted by the limited water vapor in vacuum chamber. Note that the relative durability of vapor deposition was excellent and that of dip deposition was poor. This is because when perfluorotrichlorosilane was condensed with a relatively large molecular weight, the bonding between the condensed perfluorotrichlorosilane and the substrate became relatively poor.[43]

3.1.3. Dual-Layer Coating with Plasma Treatment. Next, to achieve superoleophobicity and high durability, plasma treatment of the single layer was carried out followed by deposition of perfluorotrichlorosilane. After plasma treatment, CA of water is less than 5° on the single-layer coating, which suggested the introduction of (−OH) groups on the surface. Thickness of the vapor-deposited perfluorotrichlorosilane is approximately 300 nm. A coating of approximately 300 nm thick was initially dip-deposited on the single-layer coating using a lower concentration of perfluorotrichlorosilane (0.5 wt % in hexanes). Both wettability (CA 130° ± 2° and CAH 16° ± 2° for water, 115° ± 2° and CAH 19° ± 2° for ethylene glycol, CA 95° ± 2° and CAH 21° ± 2° for hexadecane) and durability of this coating were poor. Consequently, a thicker coating with a thickness of approximately 1 μm was deposited (2 wt % in hexanes).

As presented in Table 2, CAs of water are 166° ± 2° and 170° ± 2° for dip and vapor deposition of perfluorotrichlorosilane with the same CAH 2° ± 1°, implying superhydrophobicity. With dip deposition, CA 151° ± 4° and CAH 5° ± 3° were obtained for ethylene glycol, while CA 146° ± 3° and CAH 8° ± 2° were achieved for hexadecane; with vapor deposition, CA 165° ± 2° and CAH 3° ± 2° were obtained for ethylene glycol, while CA 153° ± 2° and CAH 4° ± 2° were achieved for hexadecane. The coatings with both deposition methods exhibited superoleophobicity. This was attributed to the existence of air cushion between the peaks of roughness features and the liquid.

The relative durability of vapor-deposited surface was excellent, whereas it was poor for dip-deposited surface. This is expected to be due to the poor adherence between the thick condensed perfluorotrichlorosilane (approximately 1 μm) and the poor bonding between the condensed perfluorotrichlorosilane and the substrate. To provide a visual illustration, the images of droplets and CAs of water (170° ± 2°), ethylene glycol (165° ± 2°), and hexadecane (153° ± 2°) on the coating produced by vapor deposition at a P−B ratio of 3.0 are shown in Figure 4.

3.2. Surface Topography and Coating Thickness. Morphological data were presented for PET substrate, single-layer coating of dip-coated PET with methylphenyl silicone

DOI: 10.1021/am5067755
ACS Appl. Mater. Interfaces 2015, 7, 743−755

resin and hydrophobic SiO_2, plasma-treated and dip-coated PET, and dual-layer coating of vapor deposition of perfluorotrichlorosilane on plasma-treated, dip-coated PET. AFM surface height maps with RMS roughness and P−V distance values are presented in Figure 5. The uncoated PET was relatively smooth (RMS = 1 ± 0.2 nm, P−V = 7 ± 3 nm). Nanoscale roughness was observed as a result of nanoparticles with binders on single-layer coating (RMS = 20 ± 2 nm, P−V = 202 ± 20 nm), single-layer coating after plasma treatment (RMS = 24 ± 2 nm, P−V = 205 ± 10 nm), and dual-layer coating (RMS = 26 ± 2 nm, P−V = 228 ± 14 nm). In dual-layer coating, the surface topography in combination with perfluorotrichlorosilane can trap more air beneath the droplets and successfully alter the hexadecane droplets from the Wenzel wetting regime (dual-layer coating without plasma treatment) to the Cassie−Baxter wetting regime (dual-layer coating with plasma treatment).[6] With a step technique, the coating thickness of the first layer was measured to be approximately 300 nm, and the coating thickness of the second layer (vapor deposition) was also approximately 300 nm as listed in Table 2.

3.3. Wear Resistance of Coated Samples. Although relative durability has been presented in Table 2, this section presents the wear data and discussion.

3.3.1. Wear on Microscale Using AFM. The results of AFM wear for single layer of dip-coated PET with methylphenyl silicone resin alone, single layer of dip-coated PET with methylphenyl silicone resin and hydrophobic SiO_2, and dual layer of vapor deposition of perfluorotrichlorosilane on plasma-treated, dip-coated PET are shown in Figure 6a. Surface height maps and surface profiles across the middle of images (locations indicated by arrows) before and after AFM wear experiment are displayed. RMS roughness and P−V distance values for surface profiles are shown within surface profile boxes.

After one cycle wear at 10 μN with the borosilicate ball, significant wear was found on single layer of dip-coated PET with methylphenyl silicone resin alone from the surface height maps along with the change of RMS and P−V value (RMS = 20 nm after compared with 11 nm before; P−V = 502 nm after compared with 380 nm before). This is due to the low hardness of methylphenyl silicone resin (1.3 GPa).[30] However, no obvious morphology change was found both on single layer of dip-coated PET with methylphenyl silicone resin and SiO_2 and on dual layer of vapor deposition of perfluorotrichlorosilane on plasma-treated, dip-coated PET after wear. The RMS and P−V values were similar before and after wear. This demonstrated that the wear resistance of dual-layer coating was superior to that of single layer of dip-coated PET with methylphenyl silicone resin alone on the microscale. Wettability of the coating after wear did not change because the wear area was small (1 μm^2) compared with contact area between liquid and the coating (0.11 mm^2 for water, 0.25 mm^2 for ethylene glycol and 0.78 mm^2 for hexadecane).

3.3.2. Wear on Macroscale Using Tribometer. The results of coated samples before and after wear experiment (locations indicated by arrows and dash lines) using ball-on-flat tribometer for single layer of dip-coated PET with methylphenyl silicone resin alone, single layer of dip-coated PET with methylphenyl silicone resin and hydrophobic SiO_2, and dual layer of vapor deposition of perfluorotrichlorosilane on plasma treated, dip-coated PET are shown in Figure 6b.

After 100 cycles wear at 10 mN, single layer of dip-coated PET with methylphenyl silicone resin alone displayed an obvious groove and showed maximum wear; single layer of dip-coated PET with methylphenyl silicone resin and SiO_2 displayed a minimum wear, and the macroscale roughness was preserved. It was observed that a small amount of coating material was rubbed off from dual-layer coating. As mentioned earlier, although the contact pressure using tribometer (4.83 MPa) is comparable to that of using AFM (10.36 MPa), higher degree of damage can be caused to the coating when multiple cycles of wear were performed, as compared to that of the AFM wear data.

To identify any changes in wettability after wear, CAs and TAs were measured on the wear track. The CAs and TAs of hexadecane droplets on the dual-layer coating after wear using ball-on-flat tribometer or scratching with tweezer are shown in Figure 7. Droplets were dragged or tilted across defect site in direction of arrows. For the coated sample before wear (left column), droplet could be dragged freely when the sample was flat with low CAH value of 4° ± 2°and the droplet rolled off at a TA of 4° ± 2°. For the coated sample after wear using ball-on-flat tribometer (center column), droplets either rolled over the defect as normal at 4° ± 2° TA when placed to the right of the defect or rolled from the defect after tilting the sample 6° ± 2° when placed directly over the defect. Droplets on the scratched sample by tweezer (right column) were pinned at the defect site until 15° ± 2° TA regardless of starting location. CAs of hexadecane droplets on all samples after wear/scratch were still greater than 150°. This indicated the superoleophobicity was preserved after wear although CAH increased slightly.

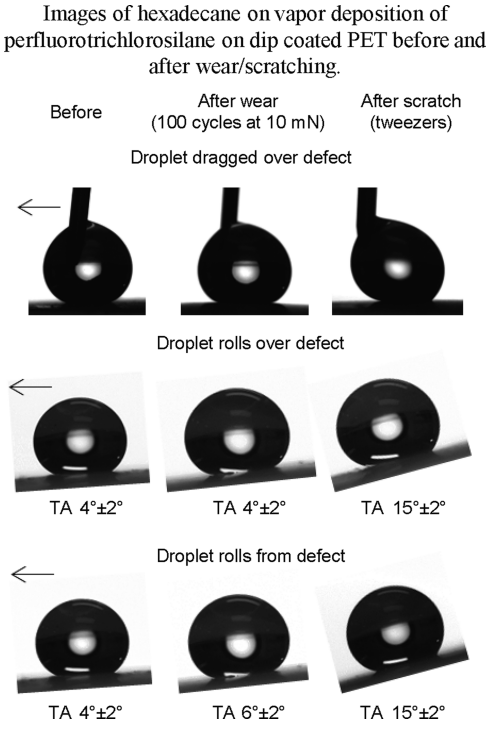

Figure 7. Images of hexadecane droplets on dual-layer coating before and after wear/scratching. Droplets were dragged or tilted across defect site in direction of arrows.

3.4. Antismudge Properties of Coated Samples. The optical micrographs of contaminated coatings and oil-impregnated microfiber cloth before and after smudge test on single layer of dip-coated PET with methylphenyl silicone resin and SiO_2 and dual layer of vapor deposition of perfluorotrichlorosilane on

DOI: 10.1021/am5067755
ACS Appl. Mater. Interfaces 2015, 7, 743−755

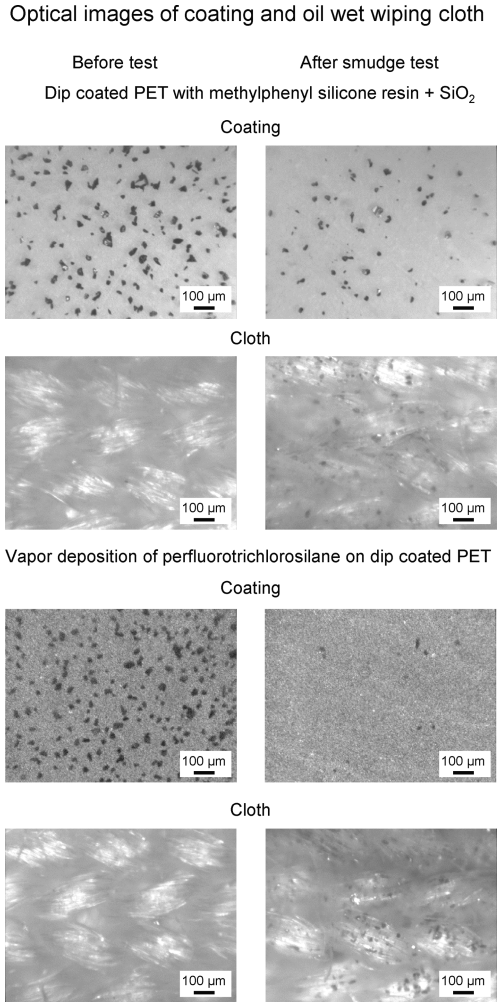

Figure 8. Optical micrographs of contaminated coatings and oil-impregnated microfiber cloth before and after smudge test on single layer of dip-coated PET and dual-layer coating.

plasma-treated, dip-coated PET are shown in Figure 8. Dark spots on coatings and cloth indicate SiC particles. It was observed that for the single-layer coating only few contaminated particles were wiped and attached to the oil-impregnated cloth, whereas for the dual-layer coating most contaminated particles were wiped off and attached to the oil-impregnated cloth. This demonstrated the antismudge properties of the dual-layer coating.

3.5. Transparency of Coated Samples. Figure 9 displays images of PET substrate, single layer of vapor deposition of perfluorotrichlorosilane on PET substrate, single layer of dip-coated PET with methylphenyl silicone resin and SiO_2, plasma-treated and dip-coated PET, and dual layer of vapor deposition of perfluorotrichlorosilane on plasma-treated, dip-coated PET showing transparency. Edges of each sample are indicated with dash line. Both single-layer coatings were as transparent as the uncoated PET substrate; the dual-layer coating was transparent, but some transparency loss was observed. It was found that the transparency of the material decreased after O_2 plasma treatment due to structural changes. Further, the thick coating (approximately 600 nm for dual-layer coating) also decreased transparency. Transparency can be improved in a future study by adjusting power and time of plasma treatment and coating thickness. Moreover, a mirrorlike appearance of the dual-layer

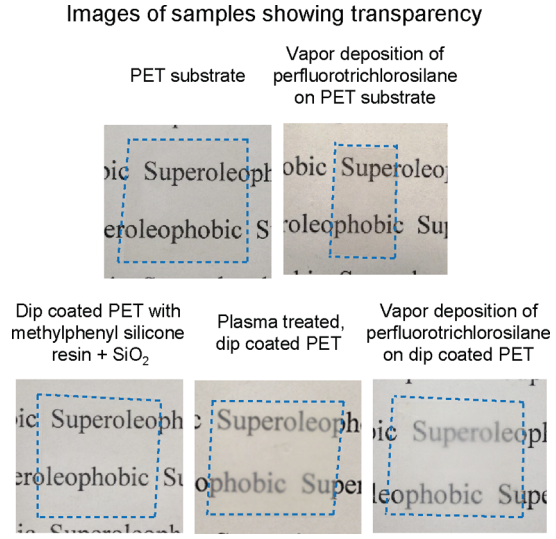

Figure 9. Photographs of samples showing transparency. Edges of each sample are shown with dash line.

coating was observed when the sample was immersed in a liquid. This is due to reduced scatter.

4. CONCLUSIONS

Superoleophobic coatings have been prepared on PET substrates by dip-coating of PET with hydrophobic SiO_2 nanoparticles and methylphenyl silicone resin, followed by O_2 plasma treatment and vapor deposition of perfluorotrichlorosilane. Methylphenyl silicone resin was selected because it provides excellent adhesion between nanoparticles and substrates and is known to be durable. Hydrophobic SiO_2 nanoparticles were selected for their high hardness and high visible transmittance, and the hydrophobic groups ($-CH_3$) can reduce the agglomeration to form a uniform coating. Perfluorotrichlorosilane was selected due to its high activity, which could hydrolyze when in contact with hydroxyl groups ($-OH$) on a surface. During coating process, plasma treatment was necessary to introduce hydroxyl groups ($-OH$) at the surface, form covalent bonds with perfluorotrichlorosilane to improve the durability, and increase coverage of perfluorotrichlorosilane to achieve superoleophobicity. Water (surface tension 72.0 mN/m) and two organic liquids, namely, ethylene glycol (48.0 mN/m) and hexadecane (27.0 mN/m), were used for CA, CAH, and TA measurements.

The P−B ratio of the first layer was optimized based on the wettability (CA/CAH/TA), and a P−B ratio of 3.0 was selected for high CA. After plasma treatment and vapor deposition of perfluorotrichlorosilane on the single layer-coating, the dual-layer coated PET surface was superoleophobic, exhibiting CA of 153° ± 2° and CAH of 4° ± 2° for hexadecane of lowest surface tension. Vapor deposition of perfluorotrichlorosilane was found to be more effective than dip deposition to obtain durable superoleophobicity.

Wear resistance of the dual-layer coating was demonstrated. Wear resistance of the coating was found to be superior to that of dip-coated PET with methylphenyl silicone resin alone both on microscale and macroscale in AFM and tribometer experiments. After wear using tribometer, CA and TA of hexadecane droplet changed to 150° ± 2° and 4° ± 2° from 153° ± 2° and 4° ± 2°. It indicated the coated surface was able to preserve the superoleophobicity after wear.

DOI: 10.1021/am5067755
ACS Appl. Mater. Interfaces 2015, 7, 743−755

Antismudge properties were also demonstrated. When the artificially contaminated coated surfaces were wiped with an oil-impregnated cloth, most contaminated particles were transferred to the wiping cloth from the dual-layer coating, while only few contaminated particles were wiped off and attached to the wiping cloth from the single-layer coating.

The coating was transparent, but some transparency was lost due to the plasma treatment and a thicker coating. This can be improved by adjusting not only the power and time of plasma treatment but also coating thickness.

In summary, superoleophobic coatings were produced on PET substrate via dip-coating and vapor-deposition methods. The antismudge properties combined with wear resistance suggest potential for industrial applications.

AUTHOR INFORMATION

Corresponding Author

*E-mail: Bhushan.2@osu.edu.

Notes

The authors declare no competing financial interest.

ACKNOWLEDGMENTS

The financial support of this research was provided in part by the National Science Foundation, Arlington, Virginia (Grant No. CMMI-1000108), and by the Dexerials Corporation, Japan (formerly Sony Corp. Chemical Division). The authors would like to thank Dr. H. Kondo and K. Yun of Dexerials Corporation for fruitful discussions. The authors would also like to thank D. Maharaj, Y. Li, and Drs. D. E. Demirocak and A. Kumar of NLBB for help and training with AFM and tribometer, and Drs. P. S. Brown and G. D. Bixler of NLBB for helpful discussions on superoleophobic coatings.

REFERENCES

(1) Hsieh, C.-T.; Chen, J.-M.; Kuo, R.-R.; Lin, T.-S.; Wu, C.-F. Influence of Surface Roughness on Water- and Oil-Repellent Surfaces Coated with Nanoparticles. *Appl. Surf. Sci.* **2005**, *240*, 318−326.

(2) Tuteja, A.; Choi, W.; Ma, M.; Mabry, J. M.; Mazzella, S. A.; Rutledge, G. C.; McKinley, G. H.; Cohen, R. E. Designing Superoleophobic Surfaces. *Science* **2007**, *318*, 1618−1622.

(3) Jung, Y. C.; Bhushan, B. Wetting Behavior of Water and Oil Droplets in Three-Phase Interfaces For Hydrophobicity/Philicity And Oleophobicity/Philicity. *Langmuir* **2009**, *25*, 14165−14173.

(4) Darmanin, T.; Guittard, F.; Amigoni, S.; Tafin de Givenchy, E.; Noblin, X.; Kofman, R.; Celestini, F. Superoleophobic Behavior of Fluorinated Conductive Polymer Films Combining Electropolymerization and Lithography. *Soft Matter* **2011**, *7*, 1053−1057.

(5) He, Z.; Ma, M.; Lan, X.; Chen, F.; Wang, K.; Deng, H.; Zhang, Q.; Fu, Q. Fabrication of a Transparent Superamphiphobic Coating with Improved Stability. *Soft Matter* **2011**, *7*, 6435−6443.

(6) Bhushan, B. *Biomimetics: Bioinspired Hierarchical-Structured Surfaces for Green Science and Technology;* Springer-Verlag: Heidelberg, Germany, 2012.

(7) Bixler, G. D.; Bhushan, B. Fluid Drag Reduction and Efficient Self-Cleaning with Rice Leaf and Butterfly Wing Bioinspired Surfaces. *Nanoscale* **2013**, *5*, 7685−7710.

(8) Muthiah, P.; Bhushan, B.; Yun, K.; Kondo, H. Dual-Layered-Coated Mechanically-Durable Superomniphobic Surfaces with Anti-Smudge Properties. *J. Colloid Interface Sci.* **2013**, *409*, 227−236.

(9) Bixler, G. D.; Theiss, A.; Bhushan, B.; Lee, S. C. Anti-Fouling Properties of Microstructured Surfaces Bio-Inspired by Rice Leaves and Butterfly Wings. *J. Colloid Interface Sci.* **2014**, *419*, 114−133.

(10) Cassie, A. B. D.; Baxter, S. Wettability of Porous Surfaces. *Trans. Faraday Soc.* **1944**, *40*, 546−551.

(11) Tsujii, K.; Yamamoto, T.; Onda, T.; Shibuichi, S. Super Oil-Repellent Surfaces. *Angew. Chem., Int. Ed. Engl.* **1997**, *36*, 1011−1012.

(12) Steele, A.; Bayer, I.; Loth, E. Inherently Superoleophobic Nanocomposite Coatings by Spray Atomization. *Nano Lett.* **2009**, *9*, 501−505.

(13) Hsieh, C.-T.; Wu, F.-L.; Chen, W.-Y. Super Water- and Oil-Repellencies From Silica-Based Nanocoatings. *Surf. Coat. Technol.* **2009**, *203*, 3377−3384.

(14) Das, A.; Schutzius, T. M.; Bayer, I. S.; Megaridis, C. M. Superoleophobic and Conductive Carbon Nanofiber/Fluoropolymer Composite Films. *Carbon* **2012**, *50*, 1346−1354.

(15) Tuteja, A.; Choi, W.; Mabry, J. M.; Mckinley, G. H.; Cohen, R. E. Robust Omniphobic Surfaces. *Proc. Natl. Acad. Sci. U. S. A.* **2008**, *105*, 18200−18205.

(16) Pan, S.; Kota, A. K.; Mabry, J. M.; Tuteja, A. Superomniphobic Surfaces for Effective Chemical Shielding. *J. Am. Chem. Soc.* **2013**, *135*, 578−581.

(17) Sheen, Y.; Huang, Y.; Liao, C.; Chou, H.; Chang, F. New Approach to Fabricate an Extremely Super-amphiphobic Surface Based on Fluorinated Silica Nanoparticles. *J. Polym. Sci., Part B: Polym. Phys.* **2008**, *46*, 1984−1990.

(18) Lovingood, D. D.; Salter, W. B.; Griffith, K. R.; Simpson, K. M.; Hearn, J. D.; Owens, J. R. Fabrication of Liquid and Vapor Protective Cotton Fabrics. *Langmuir* **2013**, *29*, 15043−15050.

(19) Han, D.; Steckl, A. J. Superhydrophobic and Oleophobic Fibers by Coaxial Electrospinning. *Langmuir* **2009**, *25*, 9454−9562.

(20) Im, M.; Im, H.; Lee, J.-H.; Yoon, J.-B.; Choi, Y.-K. A Robust Superhydrophobic and Superoleophobic Surface with Inverse-Trapezoidal Microstructures on a Large Transparent Flexible Substrate. *Soft Matter* **2010**, *6*, 1401−1404.

(21) Zhang, J.; Seeger, S. Superoleophobic Coatings with Ultralow Sliding Angles Based on Silicone Nanofilaments. *Angew. Chem., Int. Ed.* **2011**, *50*, 6652−6656.

(22) Yang, J.; Zhang, Z.; Men, X.; Xu, X.; Zhu, X. A Simple Approach to Fabricate Superoleophobic Coatings. *New J. Chem.* **2011**, *35*, 576−580.

(23) Zhao, H.; Law, K.-Y.; Sambhy, V. Fabrication, Surface Properties, and Origin of Superoleophobicity for a Model Textured Surface. *Langmuir* **2011**, *27*, 5927−5935.

(24) Deng, X.; Mammen, L.; Butt, H.-J.; Vollmer, D. Candle Soot as a Template for a Transparent Robust Superamphiphobic Coating. *Science* **2012**, *335*, 67−70.

(25) Jin, H.; Tian, X.; Ikkala, O.; Ras, R. H. A. Preservation of Superhydrophobic and Superoleophobic Properties upon Wear Damage. *ACS Appl. Mater. Interfaces* **2013**, *5*, 485−488.

(26) Bellanger, H.; Darmanin, T.; Guittard, F. Surface Structuration (Micro and/or Nano) Governed by the Fluorinated Tail Lengths toward Superoleophobic Surfaces. *Langmuir* **2012**, *28*, 186−192.

(27) Wang, X.; Hu, H.; Ye, Q.; Gao, T.; Zhou, F.; Xue, Q. Superamphiphobic Coatings with Coralline-Like Structure Enabled by One-Step Spray of Polyurethane/Carbon Nanotube Composites. *J. Mater. Chem.* **2012**, *22*, 9624−9631.

(28) Campos, R.; Guenthner, A. J.; Meuler, A. J.; Tuteja, A.; Cohen, R. E.; McKinley, G. H.; Haddad, T. S.; Mabry, J. M. Superoleophobic Surfaces through Control of Sprayed-on Stochastic Topography. *Langmuir* **2012**, *28*, 9834−9841.

(29) Ge, D.; Yang, L.; Zhang, Y.; Rahmawan, Y.; Yang, S. Transparent and Superamphiphobic Surfaces from One-Step Spray Coating of Stringed Silica Nanoparticle/Sol Solutions. *Part. Part. Syst. Charact.* **2014**, *31*, 763−770.

(30) Ebert, D.; Bhushan, B. Transparent, Superhydrophobic, and Wear-Resistant Coatings on Glass and Polymer Substrates Using SiO_2, ZnO, and ITO Nanoparticles. *Langmuir* **2012**, *28*, 11391−11399.

(31) Ebert, D.; Bhushan, B. Durable Lotus-Effect Surfaces with Hierarchical Structure Using Micro- and Nanosized Hydrophobic Silica Particles. *J. Colloid Interface Sci.* **2012**, *368*, 584−591.

(32) Bhushan, B. *Tribology and Mechanics of Magnetic Storage Devices,* 2nd ed; Springer-Verlag: New York, 1996.

DOI: 10.1021/am5067755
ACS Appl. Mater. Interfaces 2015, 7, 743−755

(33) Karunakaran, R. G.; Lu, C.-H.; Zhang, Z.; Yang, S. Highly Transparent Superhydrophobic Surfaces from the Coassembly of Nanoparticles (≤100 nm). *Langmuir* **2011**, *27*, 4594−4602.
(34) Slavov, S. V.; Sanger, A. R.; Chuang, K. T. Mechanism of Silation of Silica with Hexamethyldisilazane. *J. Phys. Chem. B* **2000**, *104*, 983−989.
(35) Bhushan, B. *Nanotribology and Nanomechanics I − Measurement Techniques and Nanomechanics, II − Nanotribology, Biomimetics, and Industrial Applications,* 3rd ed; Springer-Verlag: Heidelberg, Germany, 2011.
(36) Bhushan, B. *Introduction to Tribology,* 2nd ed; Wiley: New York, 2013.
(37) Bhushan, B.; Gupta, B. K. *Handbook of Tribology: Materials, Coatings, and Surface Treatments;* McGraw-Hill: New York, 1991.
(38) Callister, W. D.; Rethwisch, D. G. *Materials Science and Engineering—An Introduction,* 9th ed; Wiley: New York, 2013.
(39) Bhushan, B.; Muthiah, P. Anti-Smudge Screening Apparatus for Electronic Touch Screens. *Microsyst. Technol.* **2014**, *19*, 1261−1263.
(40) Jalili, M. M.; Moradian, S. Deterministic Performance Parameters for an Automotive Polyurethane Clearcoat Loaded with Hydrophilic or Hydrophobic Nano-silica. *Prog. Org. Coat.* **2009**, *66*, 359−366.
(41) Tahmasebpoor, M.; de Martín, L.; Talebi, M.; Mostoufi, N.; van Ommen, J. R. The Role of the Hydrogen Bond in Dense Nanoparticle-Gas Suspensions. *Phys. Chem. Chem. Phys.* **2013**, *15*, 5788−5793.
(42) Wenzel, R. N. Resistance of Solid Surfaces to Wetting by Water. *Ind. Eng. Chem.* **1936**, *28*, 988−994.
(43) Lee, H. J.; Owens, J. R. Design of Superhydrophobic Ultraoleophobic NyCo. *J. Mater. Sci.* **2010**, *45*, 3247−3253.
(44) Haynes, W. M. (ed.) *CRC Handbook of Chemistry and Physics,* 95th ed; CRC Press: Boca Raton, FL, 2014.

DOI: 10.1021/am5067755
ACS Appl. Mater. Interfaces 2015, 7, 743−755